Supporting Information

Visualizing interfacial charge transfer in dye sensitized nanoparticle using X-ray transient absorption spectroscopy

Xiaoyi Zhang,*[,1] Grigory Smolentsev,[3,4] Jianchang Guo,[2,#] Klaus Attenkofer,[1] Chuck Kurtz,[1] Guy Jennings,[1] Jenny V. Lockard,[2] Andrew B. Stickrath,[2] and Lin X. Chen,*[,2,5]

[1]*X-ray Sciences Division and* [2]*Chemical Sciences and Engineering Division, Argonne National Laboratory, Argonne, Illinois 60439,*

[3]*Research Center for Nanoscale Structure of Matter, Southern Federal University, Sorge 5, Rostov-na-Donu, 344090 Russia,*

[4]*Department of Chemical Physics, Lund University, P.O. Box 124, Lund, SE-22100, Sweden*

[5]*Department of Chemistry, Northwestern University, Evanston, Illinois, 60208*

[#]*current address: Chemical Sciences Division, Oak Ridge National Laboratory*

AUTHOR EMAIL ADDRESS xyzhang@aps.anl.gov; lchen@anl.gov

1. Optical transient absorption (OTA) measurement

The photo-induced electron transfer dynamics of RuN3 adsorbed to the TiO2 nanocrystalline surface has been studied intensively. A two-state electron injection model was used to describe the interfacial charge injection from photoexcited RuN3 to TiO_2 based on previous studies. (Figure S1a). The optical photon pumps RuN3 to ^{1}MLCT excited state. The

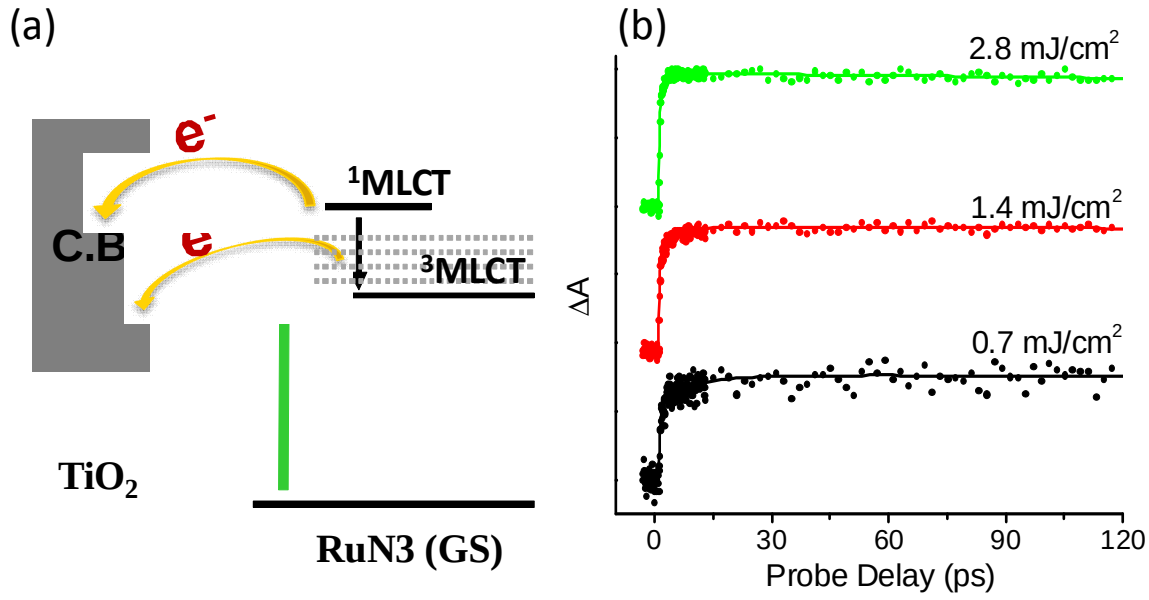

Figure S1. (a) Schematic of two-state electron injection model. (b) Optical transient absorption (OTA) kinetics probed at 910 nm at pump intensity of 0.7 mJ/cm^2 (black dots), 1.4 mJ/cm^2 (red dots), 2.8 mJ/cm^2 (green dots). The solid lines are the corresponding fittings. The absolute amplitude transient absorption was scaled for comparison purpose.

^{1}MLCT state either injects one electron to the conduction band of TiO_2 or goes to ^{3}MLCT state. The ^{3}MLCT state also injects one electron to the conduction band of TiO_2. The quantum yield of electron injection is close to 1 for 527 nm excitation.[1-3] The electron injection from ^{1}MLCT state is less than 100 fs while the electron injection from ^{3}MLCT is relatively slower; ranges from 1 ps to tens of 100 ps depending on sample environment.[4-6]

We have carried out fs optical transient absorption (OTA) measurements to measure the electron injection rates under our experimental conditions, using a Ti:Sapphire laser system as described elsewhere.[7] The optical pump pulse was 527 nm, the same pump wavelength as used in XTA measurement. The fwhm of the instrument response function was 120 fs. Figure S1b displays the kinetic traces probed at 910 nm. The transient absorption at 910 nm was assigned to the absorption of oxidized dye ($RuN3^+$) and electron in the conduction band of TiO_2 (e_{cb}^-).[8-10] We can not separate the absorption of $RuN3^+$ from e_{cb}^-. However, this shouldn't affect the measurement of the charge injection rate because $RuN3^+$ and e_{cb}^- appear as a pair. The kinetic

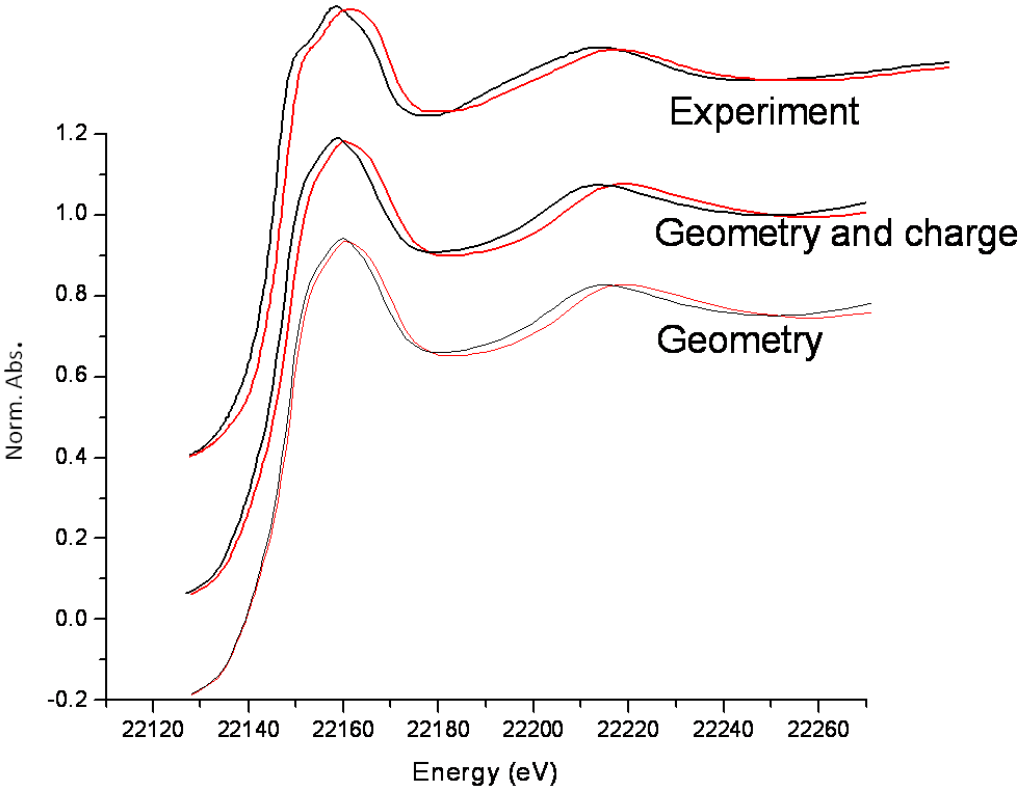

Figure S2. Comparison of experimental and theoretical XAS of $Ru^{II}(NH_3)_6^{2+}$ (black line) and $Ru^{III}(NH_3)_6^{3+}$ (red line). Calculations were performed taking into account geometrical changes only; geometrical changes and additional chemical shift of Ru^{3+} spectrum.

traces in Figure S1b were fitted to the two-state injection model[11], with a fast rise within the instrumental response function (120 fs) and a slow ps component. The slow component becomes faster as the pump intensity increases: 4 ps at 0.7 mJ/cm^2, 1.2 ps at 1.4 mJ/cm^2 and 1 ps at 2.8 mJ/cm^2. The pump intensity used in XTA is ~ 100 mJ/cm^2, therefore, we can conclude that the excited state probed by X-ray at 50 ps delay is nearly 100% $RuN3^+$.

2. Data Analysis.

The method of structure determination was based on a combination of quantitative XAS (X-ray absorption spectroscopy) fitting using the multidimensional interpolation approach[12] implemented in the FitIt code[13] and full multiple scattering (FMS) calculations of XAS using FEFF8.2[14]. The ground state spectrum was calculated from the structure obtained by X-ray diffraction (code in the CSD is XAQJOO).[15] A cluster centered at Ru atom with 5Å radius was used for the self-consistent potential calculation and that with 6Å radius was used for the FMS calculations. The energy dependent exchange-correlation potential was obtained from the Hedin-Lundqvist approach. For the photoexcited state, two structural parameters were used in the fitting: p_1 was the average Ru-N (dcbpy) distance varied within the limits 1.96-2.07 Å; p_2 was

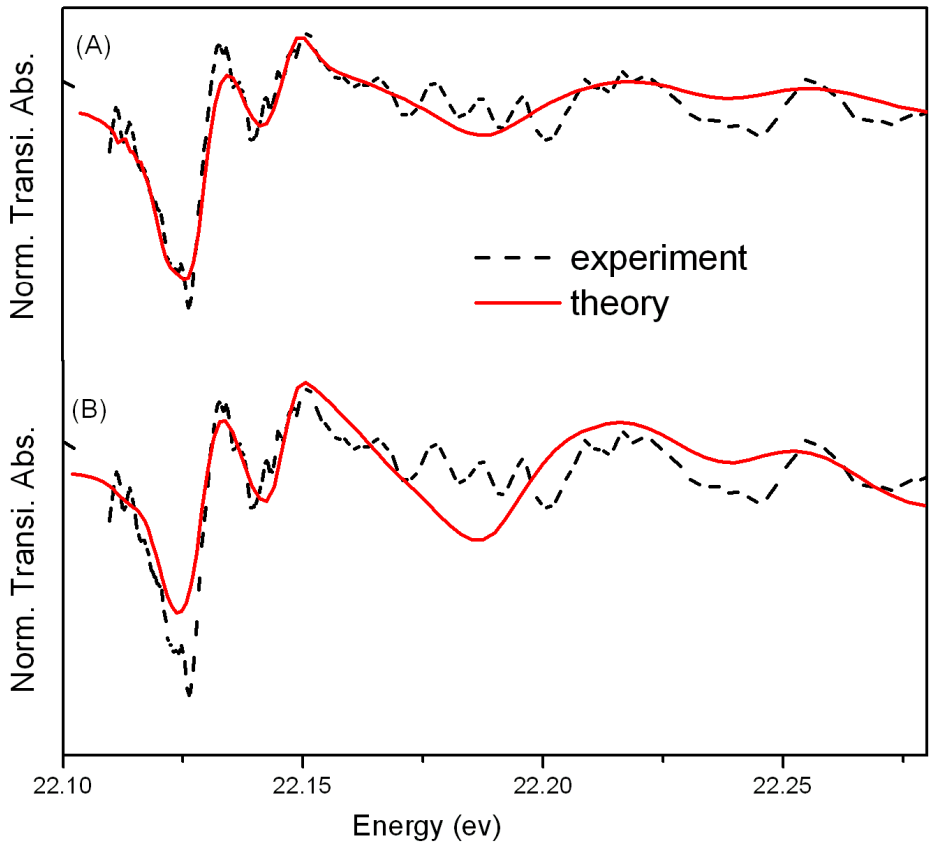

Figure S3. The transient X-ray absorption difference spectrum measured at 50 ps (black dashed line) and the calculated difference spectrum from the best fit (red curve). The calculated different spectra are (A) with 1 eV edge shift due to the charge change; (B) without taking into account of the charge effect.

the average Ru-N(NCS) distance varied between 1.89Å and 2.04Å. The ligands dcbpy and NCS were treated as rigid entities in the calculations. With the multidimensional interpolation approximation, the number of required FMS calculations for XAS spectra corresponding to different structural models was minimized by expressing the spectrum as an expansion of functions of the structural parameters. The following polynomial proved to be sufficient in our studies:

$$\mu(E, p_1 + \delta p_1, p_2 + \delta p_2) = \mu(E, p_1, p_2) + A_1(E)\delta p_1 + A_2(E)\delta p_2 + B(E)\delta p_1^2 + C(E)\delta p_1 \delta p_2$$

In order to separate the influence of geometry changes from that of the metal oxidation state changes on the XAS spectra, we performed model calculations of XAS spectra for $Ru^{II}(NH_3)_6^{2+}$ and $Ru^{III}(NH_3)_6^{3+}$ respectively with known structures.[16] The average Ru-N bond length was 2.144 Å for the former and 2.104 Å for the latter. By fixing the potential and taking into account of the geometric changes only, the edge energy shift was ~0.5 eV, whereas the experimentally observed edge shift was 1.2 - 1.5 eV, measured in a separate experiment at 10BM of the APS. Therefore, in order to mimic the influence of the oxidation state change, ~ 1eV edge shift is required to yield an XAS spectrum comparable with the experimental results. The calculated spectra of $Ru^{II}(NH_3)_6^{2+}$ and $Ru^{III}(NH_3)_6^{3+}$ agree well with the experimental measurements. (Figure S2)

We assume that the charge effect on the edge shift is also 1ev between Ru^{II}N3 and $Ru^{III}N3^+$. In the calculation of Ru^{II}N3 and $Ru^{III}N3^+$ XAS spectra, we have used a fixed potential and an additional 1eV chemical shift of the spectra. For comparison, we also fitted the difference spectrum without taking into account the edge shift caused by the change in the charge. Figure S3 compares the fitting results of the difference spectrum both with 1eV edge shift caused by the charge and without taking into account the charge effect. It is clear that the former represents a better fits to the experimental data. From the fitting obtained without the effect of the charge taken into account, the average distance between Ru and N(dcbpy) remains unchanged and the average distance between Ru and NCS has shortened by 0.09 Å in the charge separated stated as compared to the ground state. While the magnitude of the bond distance changes from the two fittings is different, the trend of the changes between Ru and the two types of ligands is the same: The average Ru-N(dcbpy) distance stays almost unchanged while the average Ru-NCS distance shrinks.

References:

(1) Eichberger, R.; Willig, F. *Chem. Phys.* **1990**, *141*, 159.

(2) Moser, J. E.; Gratzel, M. *Chimia* **1998**, *52*, 160.

(3) Nazeeruddin, M. K.; Kay, A.; Rodicio, I.; Humphry-Baker, R.; Mueller, E.; Liska, P.; Vlachopoulos, N.; Graetzel, M. *J. Am. Chem. Soc.* **1993**, *115*, 6382.

(4) Anderson, N. A.; Lian, T. Q. *Annu. Rev. Phys. Chem.* **2005**, *56*, 491.

(5) Benko, G.; Kallioinen, J.; Korppi-Tommola, J. E. I.; Yartsev, A. P.; Sundstrom, V. *J. Am. Chem. Soc.* **2002**, *124*, 489.
(6) Watson, D. F.; Meyer, G. J. *Annu. Rev. Phys. Chem.* **2005**, *56*, 119.
(7) Greenfield, S. R.; Wasielewski, M. R. *Opt. Lett.* **1995**, *20*, 1394.
(8) Das, S.; Kamat, P. V. *The Journal of Physical Chemistry B* **1998**, *102*, 8954.
(9) Rothenberger, G.; Fitzmaurice, D.; Graetzel, M. *The Journal of Physical Chemistry* **1992**, *96*, 5983.
(10) Tachibana, Y.; Moser, J. E.; Gratzel, M.; Klug, D. R.; Durrant, J. R. *Journal of Physical Chemistry* **1996**, *100*, 20056.
(11) Asbury, J. B.; Anderson, N. A.; Hao, E.; Ai, X.; Lian, T. *The Journal of Physical Chemistry B* **2003**, *107*, 7376.
(12) Smolentsev, G.; Soldatov, A. *J. Synchrot. Radiat.* **2006**, *13*, 19.
(13) Smolentsev, G.; Soldatov, A. V. *Comput. Mater. Sci.* **2007**, *39*, 569.
(14) Ankudinov, A. L.; Ravel, B.; Rehr, J. J.; Conradson, S. D. *Phys. Rev. B* **1998**, *58*, 7565.
(15) Shklover, V.; Ovchinnikov, Y. E.; Braginsky, L. S.; Zakeeruddin, S. M.; Gratzel, M. *Chemistry of Materials* **1998**, *10*, 2533.
(16) Stynes, H. C.; Ibers, J. A. *Inor. Chem.* **1971**, *10*, 2304.